

Assessment of the Intrinsic Birefringence of Partially Oriented Poly(ethylene Terephthalate) Yarns

SUNIL K. GARG, *Celanese Research Company, Box 1,000, Summit, New Jersey 07901*

Synopsis

Partially oriented poly(ethylene terephthalate) yarns (PET POY) have been studied with respect to their birefringence, sonic modulus, and stress-optical properties in an effort to extract the values for the intrinsic birefringences of the crystalline (Δn_c°) and amorphous (Δn_a°) regions. The data have been analyzed within the framework of both the sonic modulus-birefringence treatment of Samuels and Dumbleton, and the Gaussian rubber elasticity theory using the usual shrinkage stress-birefringence relations. The following values have been determined: $\Delta n_c^\circ = 0.22$ and $\Delta n_a^\circ = 0.19$. The work was undertaken to resolve the discrepancy in the published literature values of these two parameters.

INTRODUCTION

The intrinsic birefringences of the crystalline and amorphous regions Δn_c° and Δn_a° , respectively, of poly(ethylene terephthalate) (PET) have been calculated or experimentally determined by a number of authors in the past two decades.¹⁻¹² A knowledge of these two parameters is of extreme importance in attempts to correlate the mechanical properties with the structure of PET, particularly in the case of fibers and of partially oriented PET yarns (PET POY).

The various data reported in the literature have been collected together in Table I. An examination of this collection shows that considerable uncertainty attends the values both of Δn_c° and Δn_a° . It is, however, clear that except for two

TABLE I
Intrinsic Birefringence of PET

Δn_c°	Δn_a°	Reference	Comments
0.227	—	1	
0.212	—	2	Calculated
0.217	—	3	Calculated
0.216- 0.220 }	0.213- 0.216 }	4	
0.253	—	5	Calculated
0.220	0.253- 0.275 }	6	
0.22	0.20	7	
0.212	0.212	8	
0.240 } 0.251 }	0.22	9	Calculated
0.29	0.20	10	
—	0.410	11	
—	0.268	12	

calculated values for Δn_c° equal to 0.253 and 0.240–0.251 by Ikeda⁵ and Kunugi et al.,⁹ respectively, and an experimental value of 0.29 by Gupta and Kumar,¹⁰ all the other workers found Δn_c° to be 0.21–0.22, and these have been generally used by subsequent researchers.

In so far as Δn_a° is concerned, most workers have used one of the values given by Dumbleton, i.e., $\Delta n_a^\circ = 0.253$ or 0.275 ,⁶ even though various later workers, and indeed one earlier group of authors, have generally found values between 0.20–0.22. It must also be pointed out that the two most recent writings on this subject have found $\Delta n_a^\circ = 0.410$ and 0.268 as given by Harget and Oswald¹¹ and by Biangardi,¹² respectively.

The present investigation was undertaken in an attempt to reconcile the uncertainties mentioned above. We have addressed, in particular, the rather large range of the values reported for Δn_a° and have used the Gaussian rubber elasticity relations to obtain a new estimate of this parameter.

EXPERIMENTAL

Samples

The fiber samples used in this investigation were spun (melt extruded) from PET with an intrinsic viscosity of 0.64 dL/g in *o*-chlorophenol at 25°C. Extrusion temperatures ranged from 290 to 305°C and filament wind-up-speeds (WUS) ranging from 1000 to 6000 m/min were employed. Two series of fibers were prepared: (A) Fibers spun from PET containing 0.2% TiO₂, a commercial delusterant, where the filament denier (linear density) was allowed to vary with WUS. (B) Fibers spun from PET free of any additives where the filament denier was kept constant either at 3 denier/filament (dpf) or at 6 dpf. This was done to assess the effects of spinning variables and of additives on the various properties of the fibers.

Birefringence (Δn)

Birefringence of the samples was measured on a Leitz polarizing microscope with a Berek compensator. At least five readings were taken to ensure an accuracy to within ± 0.002 .

Sonic Modulus (E_s)

Sonic modulus was calculated from sonic velocity measurements made on the PPM-5 pulse propagation meter from H. Morgan Company, Cambridge, MA. The fixed load applied to the fibers to keep them parallel varied somewhat depending on the fiber linear density and WUS. In general, the loads used were low so as to impose less than 1% strain on the samples.

Density (ρ)

Densities of the fiber samples were measured in a gradient column containing calcium nitrate solutions in distilled water.

Shrinkage Force

Shrinkage force measurements were made on a device of a design similar to that described by Pinnock and Ward.¹³ Samples were clamped at constant length under a tension sufficient to keep the fibers in a essentially parallel bundle and the sample end of the device was inserted into a circulating hot air oven at 75 or 100°C. The force generated was measured using a Statham UL4-0.5 load cell and associated electronics as a function of time. The maximum in the force versus time plot, before onset of stress relaxation, was used to compute the shrinkage stress used in analysis.

Shrinkage (*S*)

The linear shrinkage of the fibers was measured in the same hot air oven at the same temperatures as the shrinkage force. The fibers were suspended vertically with a small load to keep them parallel to allow accurate and reproducible length measurements to be made. The load was, of course, much less than that required to either affect shrinkage or to draw the fibers, particularly at 100°C. The loads used were obtained through a series of independent experiments where fibers were allowed to shrink with no load and with progressively larger loads to determine the optimum load required to keep the fibers parallel but so as to not affect the length shrinkage results. The shrinkage, *S*, was calculated according to:

$$S = (L_0 - L_s)/L_0 \quad (1)$$

where L_0 is the initial length and L_s is the shrunken length of the samples.

DATA ANALYSIS

Tables II and III list the data obtained on the various samples using the techniques described above. The data were analyzed to obtain values of crystallinity, stress-optical coefficient, amorphous orientation, and related parameters as follows.

TABLE II
Properties of Series A Samples^a

Sample no.	WUS (m/min)	d _{pf}	$\Delta n \times 10^3$	$E_s \times 10^{-11}$ (dyn/cm ²)	ρ (gcm ⁻³)	$\sigma_s \times 10^{-7}$ (dyn/cm ²)	S
A-1	1500	15.4	11	0.312	1.3436	1.76	0.47
A-2	1800	12.6	16	—	1.3440	2.47	0.55
A-3	2100	11.5	21	0.333	1.3440	3.32	0.60
A-4	2400	10.1	25	—	1.3440	4.28	0.63
A-5	2750	9.4	31	0.367	1.3453	4.98	0.67
A-6	3050	8.5	38	—	1.3460	5.78	0.67
A-7	3350	7.8	48	0.468	1.3477	6.40	—
A-8	3650	7.2	57	—	1.3510	7.33	—
A-9	3950	6.6	64	0.633	1.3520	8.14	—
A-10	4300	6.3	78	—	1.3570	9.15	—
A-11	4600	5.9	85	0.828	1.3693	13.33	—
A-12	4900	5.7	95	1.008	1.3760	15.03	—
A-13	5800	5.5	112	1.165	1.3855	19.57	—

^a Extrusion temperature = 290°C; samples containing TiO₂.

TABLE III
 Properties of Series B Samples^a

Sample no.	WUS (m/min)	$\Delta n \times 10^3$	$E_c \times 10^{-11}$ (dyn/cm ²)	ρ (gcm ⁻³)
B-1	1000	10	0.285	1.3372
B-2	2000	19	0.305	1.3383
B-3	3000	40	0.389	1.3397
B-4	4000	63	0.633	1.3456
B-5	5000	71	1.031	1.3582
B-6	1000	9	0.279	1.3370
B-7	2000	20	0.322	1.3387
B-8	3000	37	0.437	1.3375
B-9	4000	55	0.656	1.3410
B-10	5000	87	1.038	1.3558
B-11	2000	37	0.372	1.3370
B-12	3000	49	0.502	1.3367
B-13	4000	64	0.763	1.3505
B-14	5000	96	1.140	1.3672

^a Samples spun from clear PET (no additives). Samples B-1 to B-5 spun with extrusion temperature = 295°C. Samples B-6 to B-14 spun with extrusion temperature = 305°C. Samples B-1 to B-10 spun with dpf = 6. Samples B-11 to B-14 spun with dpf = 3.

The fraction crystallinity, β , in these samples was obtained from the density according to the following equation:

$$\beta = \frac{\rho_c}{\rho} \left(\frac{\rho - \rho_a}{\rho_c - \rho_a} \right) \quad (2)$$

where ρ is the density of the sample, ρ_a is the density of the amorphous regions, and ρ_c is the density of the crystalline regions of PET. Some comments on the values used for ρ_a and ρ_c are necessary. The generally accepted value for $\rho_c = 1.455 \text{ gcm}^{-3}$ was given by Daubney et al.¹⁴ based on their determination of the unit cell parameters. Fakirov et al.¹⁵ have recently refined the unit cell for PET and have found a $\rho_c = 1.515 \text{ gcm}^{-3}$. In the case of PET POY, Heuvel and Huisman¹⁶ have shown that ρ_c greater than 1.455 gcm^{-3} are obtained particularly for WUS greater than 4750 m/min. It has also been found in this laboratory¹⁷ that when x-ray crystallinity is observed in PET POY samples the values calculated for ρ_c fall into two regimes: $\rho_c = 1.455 \text{ gcm}^{-3}$ for samples spun with WUS less than about 4000 m/min and $\rho_c = 1.470 \text{ gcm}^{-3}$ for samples spun with WUS greater than 4000 m/min. We have used these values in the calculation for β from eq. (2). No discontinuity in the calculated values of β was seen as a result of this procedure, see Table IV. For ρ_a the classical value equal to 1.335 gcm^{-3} has been used for the clear PET samples only. In the case of TiO_2 containing samples, the influence of this additive on the density of the amorphous regions has been taken into account since the weight fraction of the additive and its density were known. A $\rho_a = 1.341 \text{ gcm}^{-3}$ was computed through a simple additive calculation for TiO_2 containing samples and used in the calculations for β . This procedure seems justified since it is observed that, in general, the TiO_2 containing samples, series A, show a somewhat higher overall density than the samples of clear PET fibers, series B. The fraction crystallinity data are listed in Tables IV and V together with other related data for subsequent analysis.

TABLE IV
Crystallinity, Amorphous Orientation, and Derived Parameters for Series A Samples

Sample no.	β	$(1 - \beta)$	f_a ($f_c = 1$)	f_a ($f_c = 0.95$)	$\frac{\Delta n}{\beta f_c}$	$\left(\frac{1 - \beta}{\beta}\right) \frac{f_a}{f_c}$
A-1	0.025	0.975	0.10	0.10	0.44	4.02
A-2	0.028	0.972				
A-3	0.028	0.972	0.16	0.16	0.75	5.55
A-4	0.028	0.972				
A-5	0.041	0.959	0.22	0.23	0.76	5.15
A-6	0.047	0.953				
A-7	0.063	0.937	0.38	0.38	0.76	5.65
A-8	0.094	0.906				
A-9	0.093	0.907	0.52	0.53	0.69	5.07
A-10	0.134	0.866				
A-11	0.236	0.764	0.57	0.57	0.36	1.85
A-12	0.290	0.710	0.62	0.63	0.33	1.52
A-13	0.366	0.634	0.63	0.64	0.31	1.09

The chain orientation factors for the amorphous and crystalline regions in these fibers, f_a and f_c , respectively, have been obtained as follows. It is well-established¹⁶ that in the case of spun-crystallized yarns, as is the case here for samples spun with WUS greater than about 4000 m/min, f_c calculated from wide-angle x-ray measurements is close to unity, i.e., 0.95–0.98. As a result f_c has generally been equated to unity since little or no effect was found on any derived parameters when f_c in the range 0.90–1.00 were used in subsequent calculations. The chain orientation factor of the amorphous regions, f_a , was calculated from sonic modulus measurements according to the method outlined by Samuels¹⁸ and by Dumbleton,⁶ using the following relation:

$$\frac{3}{2} \frac{1}{(E_S)_{or}} = \frac{\beta(1 - f_c)}{E_{t,c}^o} + \frac{(1 - \beta)(1 - f_a)}{E_{t,a}^o} \quad (3)$$

where $(E_S)_{or}$ is the sonic modulus of the oriented sample and $E_{t,c}^o$ and $E_{t,a}^o$ are

TABLE V
Crystallinity, Amorphous Orientation, and Related Parameters for Series B Samples

Sample no.	β	$(1 - \beta)$	f_a ($f_c = 1$)	$\frac{\Delta n}{\beta f_c}$	$\left(\frac{1 - \beta}{\beta}\right) \frac{f_a}{f_c}$
B-1	0.020	0.980	0.02	0.50	0.98
B-2	0.030	0.970	0.08	0.63	2.59
B-3	0.043	0.957	0.27	0.93	6.01
B-4	0.086	0.914	0.53	0.73	5.63
B-5	0.186	0.814	0.68	0.38	2.98
B-6	0.018	0.982	0.01	0.50	0.22
B-7	0.034	0.966	0.12	0.59	3.47
B-8	0.023	0.977	0.36	1.61	15.3
B-9	0.049	0.951	0.56	1.12	10.9
B-10	0.167	0.833	0.68	0.52	3.41
B-11	0.018	0.982	0.25	2.06	13.81
B-12	0.015	0.985	0.45	3.27	29.4
B-13	0.125	0.875	0.59	0.51	4.14
B-14	0.256	0.744	0.68	0.38	1.97

the intrinsic transverse moduli of the crystalline and amorphous regions, respectively. It should be mentioned that eq. (3) was obtained by Samuels¹⁸ for polypropylene with a Poisson's ratio $\nu = 0.33$. For PET, $\nu = 0.44$,¹⁹ and the constant instead of $3/2$ would be about $1/2$. This will result in proportionate changes in $E_{t,c}^{\circ}$ and $E_{t,a}^{\circ}$ given by Dumbleton⁶ but will not affect the calculations for f_a from eq. (3). Values of f_a calculated according to eq. (3) are also listed in Tables IV and V. For comparison, values of f_a have been calculated for $f_c = 1$ and $f_c = 0.95$ in Table IV. The data are comparable in the two cases.

The shrinkage force (actually shrinkage stress) and length shrinkage data have been analyzed with the kinetic theory of rubber elasticity. This approach has been applied to PET by several workers.^{13,20-22} The essential assumptions are as follows. The fibers have been assumed to consist of a continuous amorphous matrix within which a crystalline phase is dispersed. The molecules in the amorphous regions are linked to one another to give an effectively "crosslinked" network through physical "crosslinks" such as chain entanglements and bonding forces at the amorphous-crystalline interfaces. The portions of the polymer molecules between successive "crosslinks," called the network chains, are assumed to consist of several statistical links, each made up of several monomeric repeat units. Within the framework of such a model, it may be assumed the shrinkage force developed when a PET fiber is heated to near its glass transition temperature is due entirely to the entropic recovery of the stretched, oriented chains in the amorphous region. The following relations may now be used for extracting the relevant parameters:

$$\sigma = NkT (\alpha^2 - 1/\alpha) \quad (4)$$

$$\Delta n = (2\pi/45) [(\bar{n}^2 + 2)^2/\bar{n}] \cdot N (\alpha_1 - \alpha_2) \cdot (\alpha^2 - 1/\alpha) \quad (5)$$

where σ is the stress, N is the number of network chains per cm^3 , $K = 1.38 \times 10^{-16}$ erg/K is the Boltzmann constant, T is the absolute temperature, $\alpha = 1/(1 - S)$ is the extension ratio, \bar{n} is the average refractive index of the sample, and $(\alpha_1 - \alpha_2)$ is the polarizability difference between the longitudinal and transverse axes of the samples. The stress optical coefficient (SOC) is then given by:

$$\text{SOC} = \frac{\Delta n}{\sigma} = \frac{2\pi}{45kT} \cdot \frac{(\bar{n}^2 + 2)^2}{\bar{n}} \cdot (\alpha_1 - \alpha_2) \quad (6)$$

RESULTS AND DISCUSSION

A plot of the dynamic compliance, i.e., inverse of the sonic or dynamic modulus, versus the birefringence for both series of PET POY samples are shown in Figure 1. The presence of the TiO_2 does not seem to affect the data. Data on drawn fiber samples from Dumbleton's paper⁶ have also been included in the plot. It was shown by Dumbleton⁶ that the relationship between compliance and birefringence should be a straight line with the intercept giving $E_{t,a}^{\circ}$ and the slope allowing for a calculation of Δn_a° . It is clear from Figure 1, however, that PET POY fibers do not show a straight-line behavior over the whole range of birefringences obtained during spinning. This is due to the occurrence of substantial crystallization during spinning at higher wind-up speeds. The initial part of the curve, representing essentially amorphous samples, is substantially a straight line and from a slope of this region, a $\Delta n_a^{\circ} = 0.10$ may be computed using Dumbleton's analysis.⁶

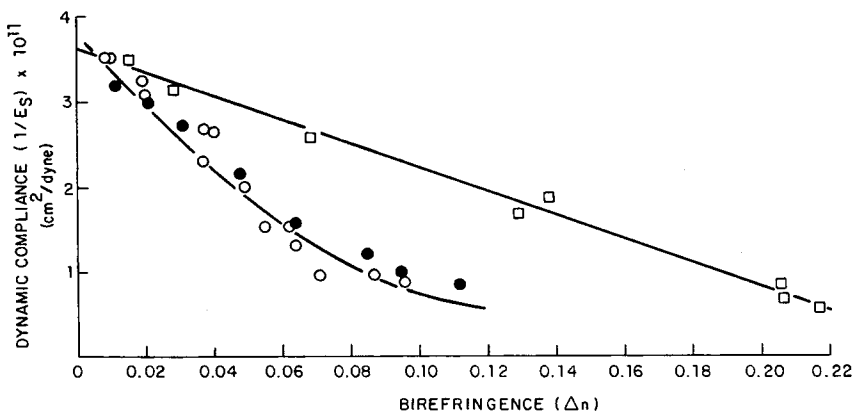


Fig. 1. Plot of dynamic (sonic) compliance vs. birefringence: (●) TiO₂ series A, (○) clear series B, (□) data from Ref. 6.

Values for Δn_a° and Δn_c° may be alternatively calculated as follows. The birefringence of an oriented fiber may be expressed by:¹⁸

$$\Delta n = \beta f_c \Delta n_c^\circ + (1 - \beta) f_a \Delta n_a^\circ \tag{7}$$

where the contributions due to form birefringence have been neglected as is usual. As a result,

$$\frac{\Delta n}{\beta f_c} = \Delta n_c^\circ + \left(\frac{1 - \beta}{\beta}\right) \frac{f_a}{f_c} \Delta n_a^\circ \tag{8}$$

All of the terms in this equation are known as outlined above, and shown in Tables IV and V, and a plot of $\Delta n/\beta f_c$ vs. $[(1 - \beta)/\beta] (f_a/f_c)$ under the assumption that $f_c = 1$ is shown in Figure 2. The intercept gives $\Delta n_c^\circ = 0.22$ while the slope gives $\Delta n_a^\circ = 0.12$. It is seen that the value for Δn_c° is in good agreement with other

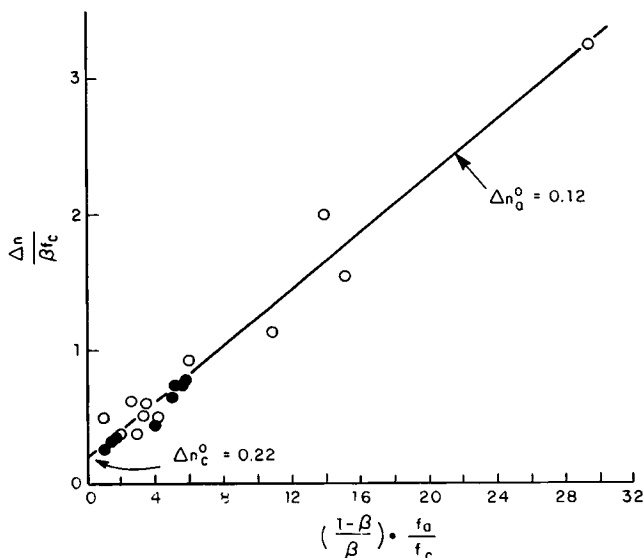


Fig. 2. Plot of $\Delta n/\beta \cdot f_c$ vs. $[(1 - \beta)/\beta] f_a/f_c$ for PET POY samples: (●) series A, (○) series B.

values reported in the literature. The value for Δn_a° , however, is much lower than values reported in the literature on drawn yarns (see Table I), but is quite in agreement with the value reported by Perez and Lecluse²³ on PET POY. This result is clearly disconcerting since any experimental methods used to calculate a universal property of PET, such as Δn_a° , should be independent of the method of sample preparation. It would also appear that the essential model used in calculating f_a from sonic modulus measurements may not apply universally to PET samples prepared under various conditions. It should be pointed out that Ward^{19,24} has shown that the linear relationship between sonic modulus and birefringence may be rigorously derived only for samples of low overall orientation. As DeVries et al.⁷ have pointed out, Dumbleton's⁶ essential conclusions with regards to $\Delta n_a^\circ = 0.253$ were reached on the basis of a linear extrapolation of a graph of sonic compliance versus birefringence, the highest measured value of birefringence being 0.138. This relationship is, however, not necessarily linear for all types of samples (see Fig. 1), and a deviation from linearity at high orientations would certainly complicate this type of analysis.

Shrinkage stress and length shrinkage measurements on essentially amorphous yarns were used, as a result, as an alternate technique to assess Δn_a° . This was done, in particular, since a considerable amount of data exist on stress-optical properties of PET, both on as-spun fibers and on drawn fibers and films,^{13,20-22} to allow for an adequate comparison between samples prepared under various conditions. A plot of birefringence, Δn , versus the shrinkage stress, σ_s , of series A samples is shown in Figure 3. From the initial linear portion of the plot a stress-optical coefficient (SOC = $\Delta n/\sigma_s$) of 6.4×10^{-10} cm²/dyn was calculated. The departure from linearity in this plot may be attributed either to the presence of substantial (> 5%) crystallinity in the samples or to the presence of sufficient amounts of highly oriented and rapidly crystallizable amorphous regions. Pinnock and Ward¹³ obtained a value for SOC = 5.5×10^{-10} cm²/dyn on low-speed spun PET fibers. Rietsch et al.²¹ have shown that SOC calculated from drawn films also has a similar value. Moreover, their data on drawn films show a behavior essentially identical with the data on PET POY, see Figure 3. It would appear then that the SOC is relatively insensitive to the method of sample preparation.

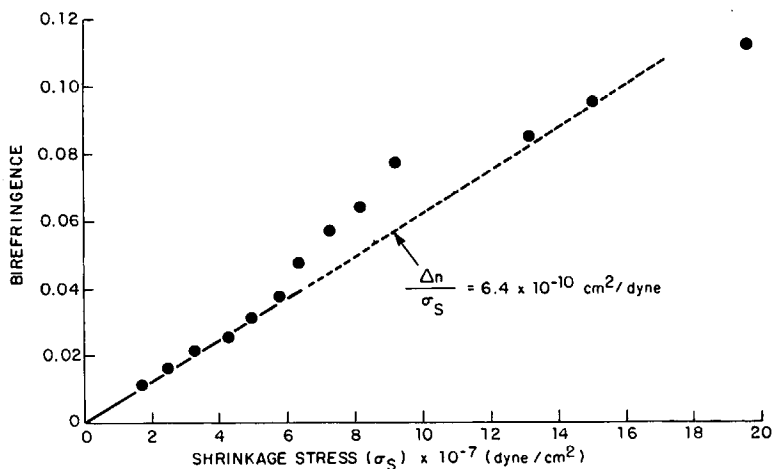


Fig. 3. Birefringence vs. shrinkage stress for series A PET POY samples at 75°C.

It should be noted that in a study of the thermal shrinkage of drawn PET filaments, Bhatt and Bell²² found SOC to be 10.45×10^{-10} cm²/dyn. An examination of their data reveals, however, that the samples examined by them fall in the Δn range of 0.54–0.210 and that both the present data and the data of Ward et al.²¹ indicate a significant change in the slope of the Δn vs. σ_s curve above a Δn of about 0.030. If SOC were to be calculated from the data above $\Delta n \approx 0.030$ in Figure 3, a value almost as high as that given by Bhatt and Bell²² may be computed. We feel, however, that in the range studied by them the assumptions of Gaussian rubber elasticity theory no longer apply mainly due to the presence of too large a fraction of crystals in the material.

The intrinsic birefringence of the amorphous regions, Δn_a° , may be computed from:²²

$$\Delta n_a^\circ = N n (\alpha_1 - \alpha_2) (4\pi/3) [(\bar{n}^2 + 2)^2/6\bar{n}] \quad (9)$$

The principal polarizability difference ($\alpha_1 - \alpha_2$) may be computed from the SOC [eq. (6)] using $\bar{n} = 1.575$ to give a value of 1.72×10^{-23} cm⁻³. The value of N , the number of network chains, may be computed from eqs. (4) and (5) by plotting either σ_s or Δn vs. $(\alpha^2 - 1/\alpha)$. Plots of σ_s vs. $(\alpha^2 - 1/\alpha)$ and Δn vs. $(\alpha^2 - 1/\alpha)$ are shown in Figure 4 and both plots give $N = 1.10 \times 10^{20}$ cm⁻³. The polarizability of a fully extended PET monomer unit is 0.52×10^{-23} cm⁻³, and as a result, if the unit in the rubber-like network assumed here were also fully extended, then there would be 3.3 monomer units per statistical link.¹³ Using an amorphous density for PET of 1.335 with the value obtained above for N , the number of network chains, it may be shown that the number of monomers per network chain is 38.4. A division of the number of monomers per network chains by the number of monomer units per statistical link gives a value of 11.5 for n , the number of statistical segments per network chain.²² A calculation using eq. (9) there gives $\Delta n_a^\circ = 0.190$. Similar calculations based on the data of Pinnock and Ward¹³ and of Reitsch et al.²¹ lead to $\Delta n_a^\circ = 0.192$ –0.194. The data of Bhatt and

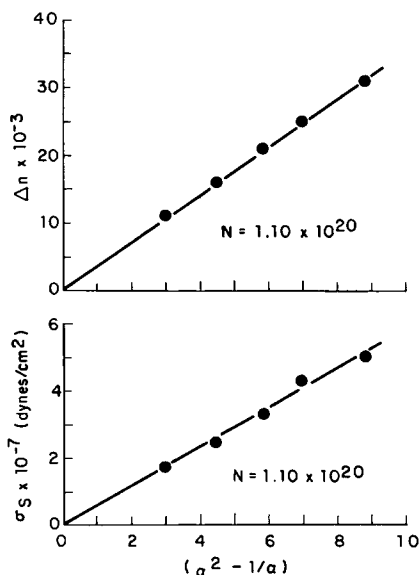


Fig. 4. Plots according to eqs. (4) (bottom) and (5) (top) for PET POY samples.

Bell²² lead to a much higher value of Δn_a° due mainly to the much higher SOC that was obtained initially.

It should be mentioned that the value of Δn_a° computed using thermal shrinkage measurements is insensitive to the method of preparation of the samples used and, additionally, on the experimentally determined value of SOC. Furthermore, while the calculated values of the number of statistical links in the rubber-like network, the number of monomer units per statistical link, and the number of network chains all depend on the molecular weight of the PET used in sample preparation,¹³ the value of Δn_a° calculated according to the procedure outlined above does not.

CONCLUSIONS

It has been shown that the intrinsic birefringences of the crystalline and amorphous regions of PET, Δn_c° and Δn_a° are 0.22 and 0.19, respectively. The Δn_c° obtained in this work is close to that generally used in the literature and obtained by most other workers, see Table I. The value for Δn_a° , however, is somewhat smaller than the normally accepted value of 0.275.⁶

It was found, additionally, that the analysis of the data within the framework presented in this paper was insensitive to the wide range of spinning conditions used to prepare the sample studied. It is believed, however, that the former (0.19) value obtained through thermal shrinkage measurements is more representative of the Δn_a° for PET. This is so since similar values are obtained on samples oriented in a variety of ways such as spinning partially oriented filaments over a wide range of conditions, by spinning and drawing of filaments, or by tensile drawing of PET films. This does not seem to be the case with the sonic modulus method employed by Dumbleton⁶ to obtain the higher (0.275) value for Δn_a° where, it has been shown, the calculations for the orientation of the amorphous regions are model dependent and differing values for Δn_a° are obtained from samples prepared by different methods.

With regards to the very high value for Δn_a° (equal to 0.410) calculated by Harget and Oswald¹¹ from x-ray measurements, it has already been shown¹² that this was based on a wrong calculation for $\langle \text{COS}^2 \theta \rangle$, a term related to the orientation distribution function of chain segments.

Biangardi¹² has also calculated a value for Δn_a° from an analysis of the orientation distribution function of the chain segments in amorphous PET obtained using wide-angle x-ray scattering. Essentially, the method involved the use of a plot of the Hermans orientation factor for the amorphous regions, f_a (f_a is related to the orientation distribution function), versus the birefringence, Δn , of the fiber samples used. The range of f_a of the samples used was 0–0.25 while the range of Δn was 0–0.060. A linear extrapolation to $f_a = 1$ (perfect chain orientation) was carried out and a value of $\Delta n_a^\circ = 0.268$ was obtained. It has, however, been shown by Zachmann²⁵ that the relationship between f_a and Δn , for PET, is nonlinear for values of f_a and Δn greater than about 0.60 and 0.060, respectively. This latter result, we feel, renders Biangardi's¹² linear extrapolation to $f_a = 1$ nebulous, at best.

The author would like to extend his thanks to Dr. R. M. Mininni for discussions during the course of this work. Jane Scott, Foster Warner, and Robert Roschen assisted in collection of the data analyzed in this paper.

References

1. D. Patterson and I. M. Ward, *Trans. Faraday Soc.*, **53**, 1516 (1957).
2. G. Farrow and J. Bagley, *Text. Res. J.*, **32**, 587 (1962).
3. I. Kuriyama, K. Tomita, and K. Shirakashi, *Sen'i Gakkaishi*, **20**, 431 (1964).
4. S. Okajima and K. Kayama, *Sen'i Gakkaishi*, **22**, 51 (1966).
5. M. Ikeda, *Sen'i Gakkaishi*, **23**, 418 (1967).
6. J. H. Dumbleton, *J. Polym. Sci., A-2*, **6**, 795 (1968).
7. A. J. DeVries, C. Bonnebat, and J. Beutemps, *J. Polym. Sci., Polym. Symp. C*, **58**, 109 (1977).
8. A. Konda, K. Nose, and H. Ishikawa, *J. Polym. Sci., A-2*, **14**, 1495 (1976).
9. T. Kunugi, K. Shiratori, K. Uematsu, and M. Hashimoto, *Polymer*, **20**, 171 (1979).
10. V. B. Gupta and S. Kumar, *J. Polym. Sci., Polym. Phys. Ed.*, **17**, 1307 (1979).
11. P. J. Harget and H. J. Oswald, *J. Polym. Sci., Polym. Phys. Ed.*, **17**, 531 (1979).
12. H. J. Biangardi, *J. Polym. Sci., Polym. Phys. Ed.*, **18**, 903 (1980).
13. P. R. Pinnock and I. M. Ward, *Trans. Faraday Soc.*, **62**, 1308 (1966).
14. R. de P. Daubney, C. W. Bunn, and C. J. Brown, *Proc. R. Soc. A*, **226**, 531 (1954).
15. S. Fakirov, E. W. Fischer, and G. F. Schmidt, *Makromol. Chem.*, **176**, 2459 (1975).
16. H. M. Heuvel and R. Huisman, *J. Appl. Polym. Sci.*, **22**, 2229 (1978).
17. S. K. Garg, unpublished work.
18. R. J. Samuels, *J. Polym. Sci., Part A*, **3**, 1741 (1965).
19. I. M. Ward, *Mechanical Properties of Solid Polymers*, Wiley, New York, 1971.
20. J. H. Dumbleton, *Text. Res. J.*, **70**, 1035 (1970).
21. F. Reitsch, R.A. Duckett, and I. M. Ward, *Polymer*, **20**, 1133 (1979).
22. G. M. Bhatt and J. P. Bell, *J. Polym. Sci., Polym. Phys. Ed.*, **14**, 575 (1976).
23. G. Perez and C. Lecluse, *18 Internationale Chemiefasertagung in Dornbirn*, 1979, Vol. 20, No. 22.
24. I. M. Ward, *Text. Res. J.*, **34**, 806 (1964).
25. H. G. Zachmann, *Polym. Eng. Sci.*, **19**, 966 (1979).

Received November 18, 1981

Accepted January 18, 1982